Effects of Earthquakes on Hydrothermal Vent Temperature and Resistivity at the Main Endeavor Field, Northeast Pacific

Stephen Mylett

University of Washington
School of Oceanography, Box 357940
Seattle, WA 98195-7940

Email: Myl3tt91@uw.edu

Plain Language Summary

This proposed research will examine the aftereffects of earthquakes on hydrothermal vent temperature and resistivity, off the coast of WA and Vancouver Island, BC. The results of this research and its conclusion will help gain a better understanding of the severity of temperature and resistivity fluctuations at vents due to earthquakes. Data collected by similar, previous research, indicates earthquakes do play a role in changing properties of vents and this research will be a continuation of this topic. With use of newer implemented instruments near the target vents, and UW compiled earthquake catalogue, cross referencing collected data between July 2017 – May 2019 and April 2019 – August 2019 and determining the severity of temperature and resistivity response to seismic activity was possible. Additionally, these effects may pose a threat to the survivability of the surrounding biological communities.

Abstract

Hydrothermal vents are important deep ocean structures that provides a necessary biogeochemical environment which supports life. The flux of high temperature vent fluid, via hydrothermal circulation, mixes with cooler ocean water and increases pH since vent fluid is acidic, which enables precipitation of important molecules like iron sulfide and manganese. The hydrothermal circulation process consists of seawater entering permeable fractures surrounding vents and reaching the reaction zone, just above the magma chamber in Layer 3 of the oceanic lithosphere, which is the lower section of the oceanic lithosphere and upper mantle. The interaction of seawater and magma adds Fe, Mg, Si, Al, Ca, S, and other elements to this fluid mixture. Once temperature and pressure reach a certain point in Layer 3, the fluid is be expelled

back into the ocean and disseminates the newly formed elements into surrounding seawater. The addition of the elements then creates a habitable environment that supports life at the extreme depths where the vents form. The purpose of this research and analysis, was to determine whether earthquake activity affects hydrothermal vent temperature and resistivity in the Main Endeavour Field (MEF) on the Juan de Fuca Ridge, off the coast of Washington State and Vancouver Island, BC, between July 2017 – May 2019 and April 2019 – August 2019. Using Ocean Network Canada (ONC) data and a University of Washington (UW) compiled earthquake catalogue, the earthquake frequency, magnitude, and moment were compared to fluctuating temperature and resistivity at MEF. It seems temperature and resistivity are affected by seismic activity; however, other factors may need to be taken into consideration. After major earthquake events, temperature steadily increases over a span of a few months and resistivity fluctuates to max and min values rapidly. Understanding how temperature and resistivity responds to seismic activity will help determine secondary effects on properties such as salinity, volatile species, and any organisms living near these vents.

Introduction

Hydrothermal vents are underwater fissures that are formed by expelled magma, or partial melt, which then cools once it encounters colder seawater. Through the process of the magma expulsion, important volatile species are brought to the surface within the melt. These properties create a habitable environment that supports life at the extreme depths where the vents form. Additionally, the interaction between the melt and seawater will change the temperature, resistivity, and overall habitability of the surrounding seawater. Depending on the type of vent, temperatures of the fluid can range from 300 ^{o}C to 400 ^{o}C, while surrounding seawater is ~ 2 ^{o}C

at the same depths. Because of the temperature and compositional differences, the fluid will then interact one more time with seawater. This interaction provides fluctuations in volatile species and can create precipitates that are necessary for the surrounding biological communities which consist of bacteria, archaea, and organisms such as tubeworms. These organisms live off the nutrients and precipitates from vents since there is no light at such depths. (Tsurumi & Tunnicliffe, 2003; Kelley et al., 2012). Although vent fluid discharge is necessary for surrounding life, if earthquake activity does have a direct influence on temperature and resistivity, then increased earthquake activity may lead to unfavorable temperature and resistivity conditions for surrounding life.

MEF, Fig. 1 & 2, is in the northern portion of the Juan de Fuca Ridge which is located in the northeastern portion of the Pacific, off the coast of WA and Vancouver Island, BC. The MEF houses multiple active hydrothermal fields (Kelley et al., 2012), and has been recognized as an area where seismic intensity directly effects individual vent temperatures (Wilcock et al., 2007; Kellogg, 2011). Unlike hydrothermal vents at different locations such as the Aurora vent field off the coast of Greenland, or the Eye of Mordor on the Galapagos Rift (http://vents-data.interridge.org/ventfields), the MEF is a confirmed active vent field with a highly capable cabled observatory, the Northeast Pacific Time-Series Underwater Experiment (NEPTUNE), that has already been established. Additionally, seismometers within NEPTUNE have and are recording seismic activity. These reasons are why MEF was an ideal location for this study. The implementation of NEPTUNE provided a high-bandwidth underwater cable observatory and aided in the ability to survey hydrothermal vents in the Endeavour segment (Kelley et al., 2012).

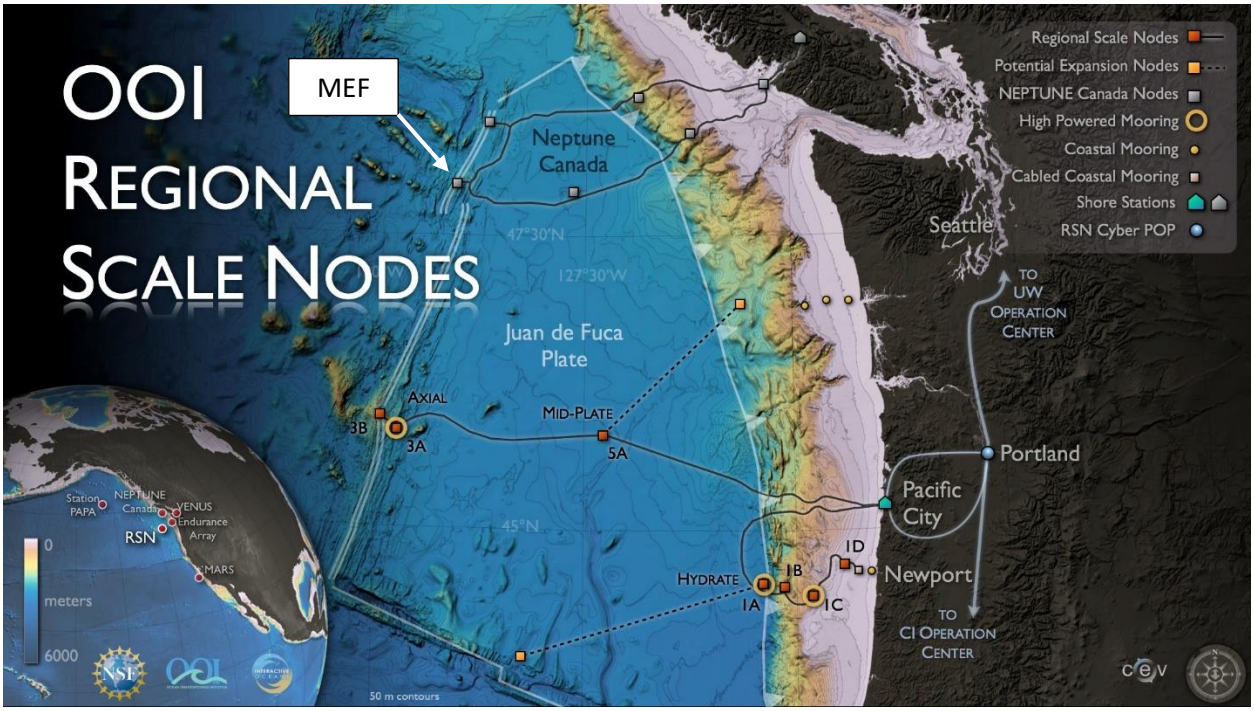

Figure 1: Map of Neptune Cabled Observatory with MEF, location of study, emphasized. The original image was produced by Ocean Network Canada.

Although this topic has been studied in the past, the ability to compare two sets of data so closely from the same vent field had not been possible until the installation of NEPTUNE in 2009. One important research effort was conducted between 1999 – 2000. This field effort began with the detection of recent increased seismic activity at the MEF and proved to be a good opportunity to see if and how this would influence volatile species and temperature (Seewald et al., 2003). Meanwhile, pre-earthquake properties were also being compared to post-earthquake activity. The scientists measured temperatures and collected fluid samples at several hydrothermal vents to measure any concentration changes in volatile species they were focused toward. These species included H_2, H_2S, CH_4, CO_2, NH_3, Mg and Cl (Seewald et al., 2003). Analyses was conducted within hours of subsurface retrieval of samples, and they found dissolved concentrations of CO_2, H_2, and H_2S increased post-earthquakes. Simultaneously, NH_3

and CH_4 concentrations that remained were less than pre-earthquake activity or around the same (Seewald et al., 2003). Chlorinity showed to have had a rapid decrease in concentration with a quick rebound back to original concentration (Seewald et al., 2003). Additionally, temperature had increased after seismic activity. Table 1 shows how some of the concentrations of gases fluctuated between 1999 – 2000. Most of the studied gasses rebounded back to normal. It was pointed out that there were some uncertainties in their fluid samples due to seawater entrainment while subsurface retrieving (Seewald et al. 2003).

Table 1: Measured abundances and extrapolated endmember concentrations of dissolved gases, Cl, and Mg in hydrothermal fluids collected from the Main Endeavour Field. Table from (Ding et al., 2001)

Vent-Year	Sample	Structure	Temperature (°C)	H_2 (mmol/l)	H_2S (mmol/l)	CH_4 (mmol/l)	CO_2 (mmol/kg)	NH_3 (µmol/kg)
Hulk-1999	M3468A	Flange	339	na	2.8	na	na	159
	M3468B	Flange	339	na	6.2	na	na	411
	M3468C	Chimney	341	na	6.5	na	na	499
	M3468D	Chimney	341	na	6.0	na	na	493
	BGT3478	Flange	347	0.31	7.0	1.4	51	479
	Endmember			0.33	7.4	1.6	53	503
Hulk-2000	BGT-3591-2	Chimney	na	0.20	5.3	1.4	26.5	420
	BGT-3591-3	Flange	120	0.083	1.9	0.5	11.9	122
	BGT-3591-4	Flange	120	0.076	1.7	0.49	10.8	122
	Endmember			0.23	5.8	1.5	29	447
Dante-1999	M3470A	Flange	350	na	7.8	na	na	398
	M3470B	Flange	350	na	11	na	na	383
	Endmember			0.52[a]	13	na	na	529
Dante-2000	BGT-3590-2	Flange	341	0.29	7.3	1.3	26.0	418
	BGT-3590-3	Flange	341	0.27	8.9	1.3	23.9	415
	BGT-3590-4	Flange	341	0.28	7.3	1.3	23.9	426

Knowing that there has been proven influences on temperature and volatile species via earthquake activity from past research, temperature increase can be expected at the end of this research. Additionally, using data that has already been collected between the July 2017 – April 2019 and April 2019 – August 2019 will provide a way to look at more than a single earthquake event. These two timelines will allow an extended look at temperature fluctuations, effects on resistivity, and the severity of which earthquakes affect these two properties.

Methods

For this project, two sets of data were used which included temperature and resistivity data and an earthquake catalogue. The location where research of earthquake effects on vent temperature and resistivity was conducted at MEF, which is the western most section of NEPTUNE (Fig. 2). The temperature and resistivity data were originally collected via a benthic and resistivity sensor (BARS). Temperature data came from the northern BARS at 47.9493°N, -129.095°W, and the resistivity data came from the southern BARS at 47.9481°N, -129.0986°W. Since there were gaps in temperature and resistivity data, both BARS were used to provide continuous data. The northern and southern BARS are ~0.13 km away from each other.

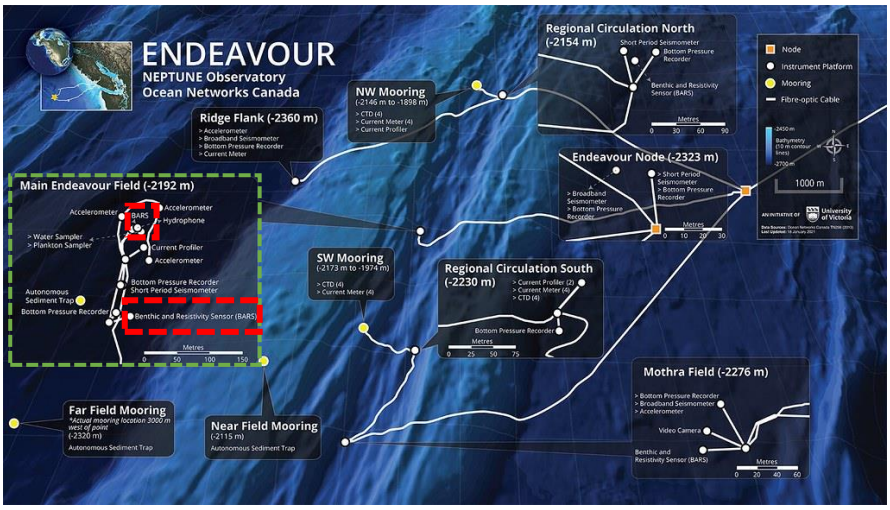

Figure 2: Zoomed in map of Neptune Cabled Observatory. MEF is highlighted in the green dashed square. The highlighted red boxes show the location of the two BARS used for this research. The original image was produced by Ocean Network Canada.

All the temperature data from the two locations were downloaded from ONC's website. (https://data.oceannetworks.ca/PlottingUtility, January 2021). The earthquake data used was collected, calculated, compiled, and disseminated by Zoe Krauss, graduate student at University of Washington – School of Oceanography. This data file included daily earthquake occurrences, latitude/longitude, magnitude, moment, depth, and distance away from MEF between July 2016 and January 2021.

Using the earthquake catalogue, histograms of quake cumulative moment over time, number of events per day, and daily moment sum were generated through Python. The histograms were plotted with all available data and the restricted timeline, July 2017 – April 2019 and April 2019 – August 2019. Once the histograms were completed, the downloaded data from ONC was placed side-by-side to look for relationships and any noticeable patterns.

Results:

The long-term temperature record has large data gaps between 2010 to 2017 (Fig. 4). Continuous temperature data began late 2017. From July 2017 – January 2018, temperature remained between 335°C – 340°C. Beginning in 2018, the vent temperature decreases ~ 20°C over the span of a month. Temperature remains between

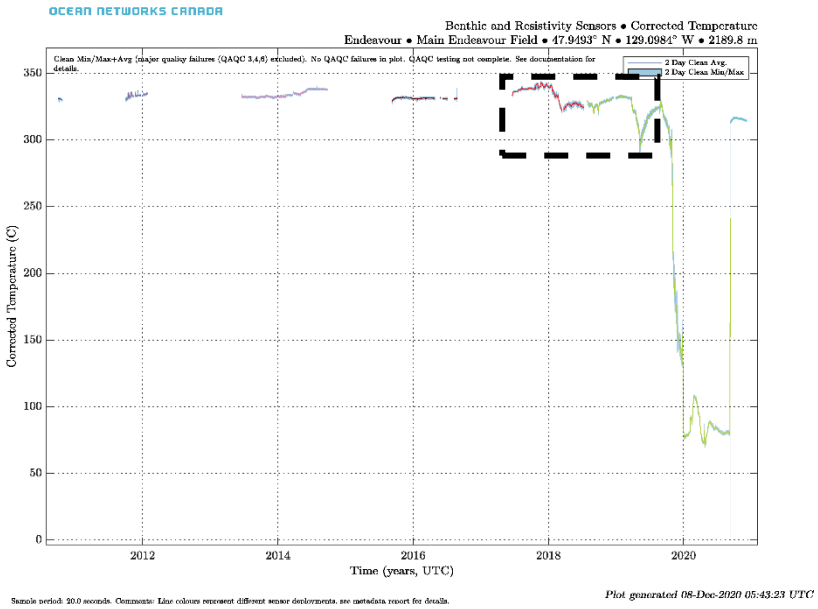

Figure 4: All temperature data available from BARS. This data and plot were collected and generated by Ocean Networks Canada. Black dashed box is the time-period used in this study.

322ºC – 332ºC until April 2019 when the temperature decreases ~35ºC. Temperature remained at this lower temperature for a few days, then began to rise back up ~35ºC over the next two and a half months (Fig. 5). Once temperature reached its max of ~325ºC at the beginning of September 2019, it fell to ~75ºC by the January 2020. Temperature then immediately increases from 75ºC to 325ºC in the span of a day during September 2020. (Fig. 6).

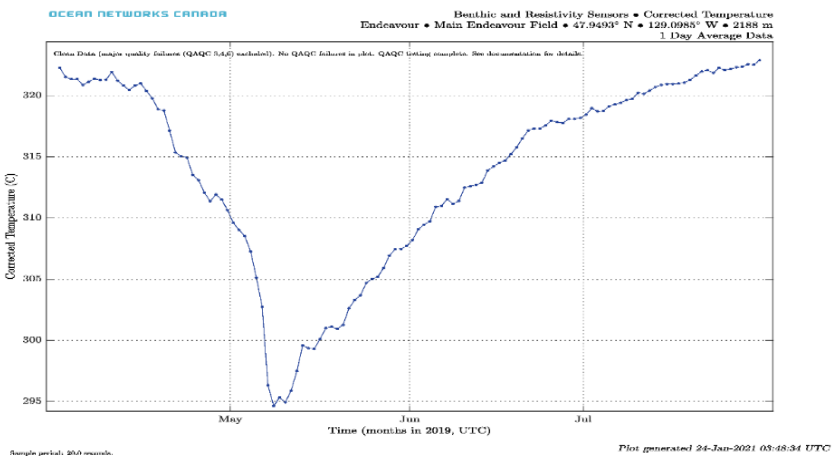

Figure 5: Temperature daily averages from BARS between April 1, 2019 to August 1, 2019. Data and plot were collected and generated by Ocean Networks Canada.

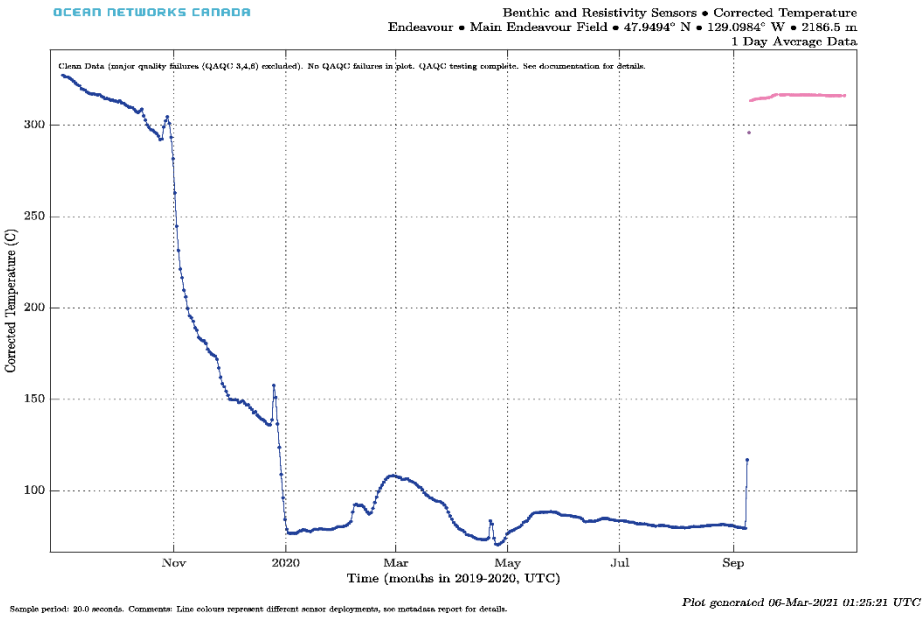

Figure 6: Temperature daily averages from BARS between September 1, 2019 to November 1, 2020. Data and plot were collected and generated by Ocean Networks Canada.

The overall resistivity plot, from the southern BARS, is missing data from 2010 – early 2018 (Fig 7). Once resistivity data becomes reliable in mid-2017, voltage begins to increase from 0 volts (V) – 1 V (Fig. 8). Voltage then gradually decreases ~0.4 V until January 2019. At the beginning of January 2019, voltage immediately increases to 0.8 V in the span of a few days. Voltage averages ~0.8 V until mid-March. During that time, voltage gradually increased to ~1.1 V to the beginning of April,

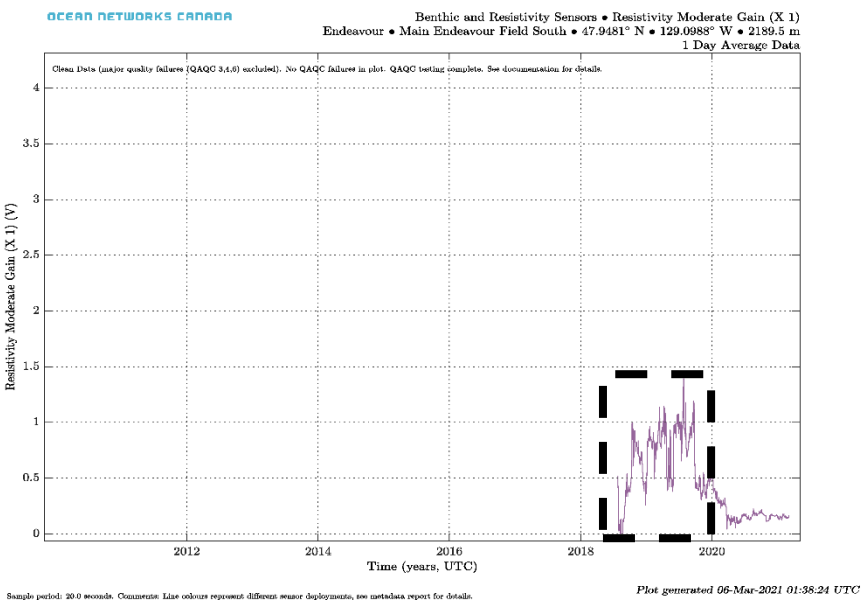

Figure 7: All resistivity data collected from BARS South. This data and plot were collected and generated by Ocean Networks Canada. Black dashed box is the time-period used in this study.

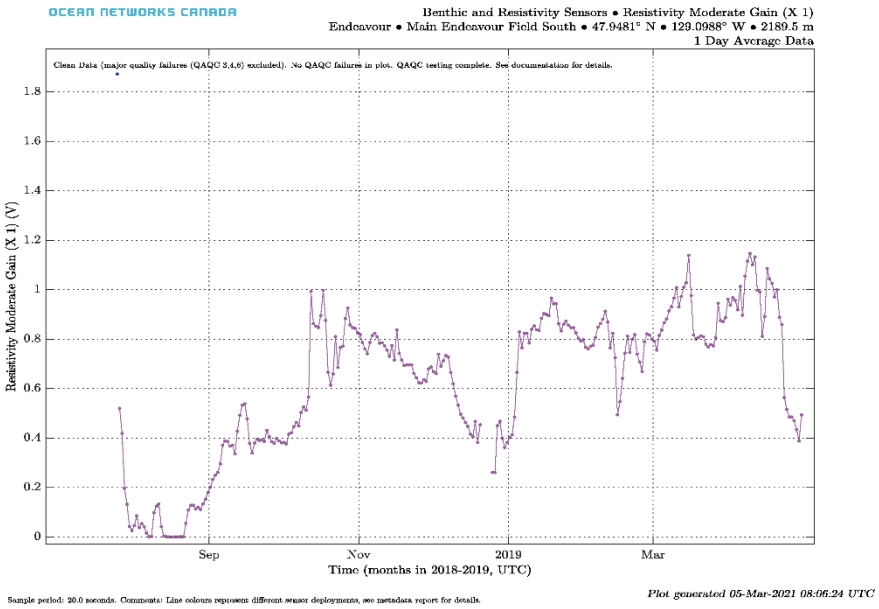

Figure 8: Resistivity daily averages between July 2017 – April 2019. This data and plot were collected and generated by Ocean Networks Canada

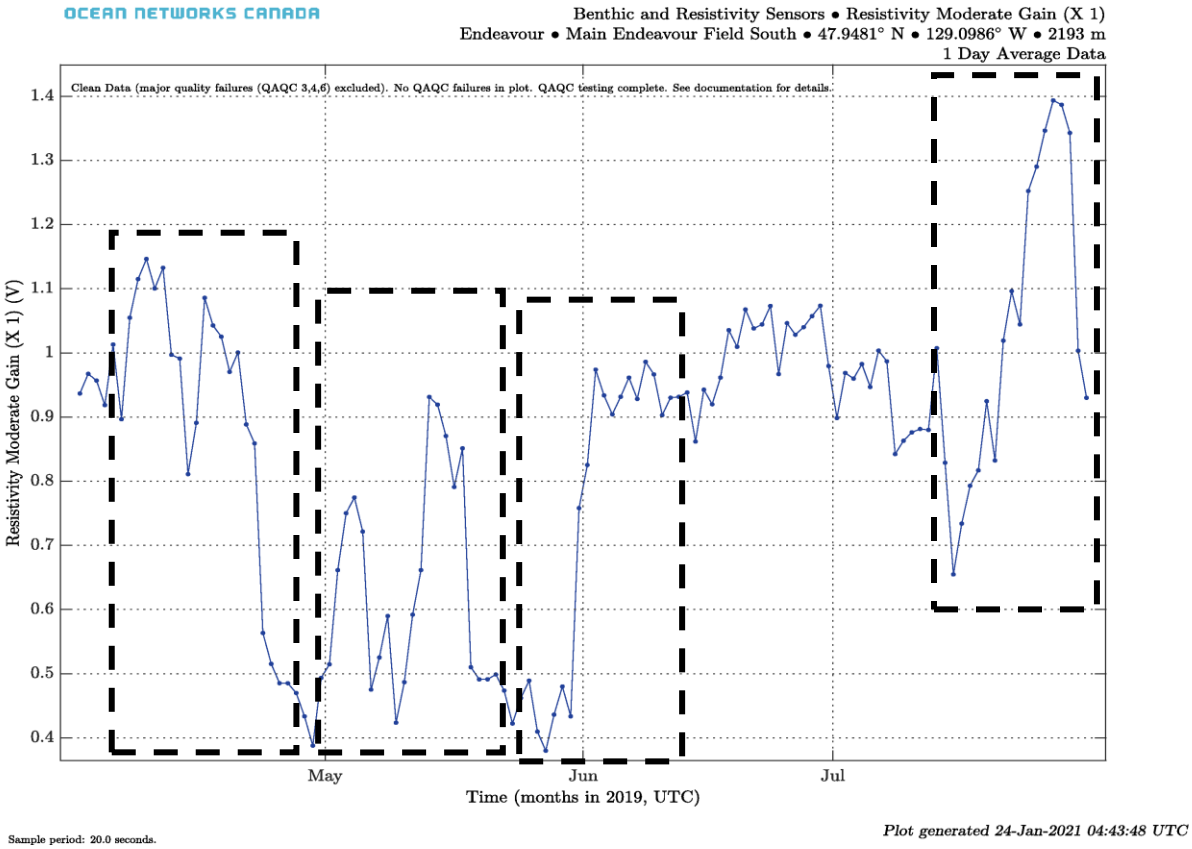

Figure 9: Resistivity daily averages from BARS between April 1, 2019 to August 1, 2019. Data and plot were collected and generated by Ocean Networks Canada. Four dashed boxes emphasize the major voltage changes.

then immediately dropped back down to 0.8 V in a few days. Several weeks after that drop, resistivity again increased back up to ~1.1 V and fluctuated up and down for another week. Resistivity then decreased down to ~0.4 V from April 2019 into May 2019. The resistivity then increased from 0.4 V to 0.9 V in mid-May then returned to 0.4 V a few days later (Fig. 9). Voltage increased from 0.45 V to 0.98 V over the course of a day and remained near that voltage till mid-July. Mid-July, resistivity increased to 1.4 V, then almost immediately decreased back to ~0.9 V (Fig.9).

The overall earthquake plot between July 2016 – January 2021 shows four separate sections, emphasized by the blue brackets, where earthquake occurred more frequently than other sections (Fig. 10). Additionally, there are two noticeable spikes in the Daily Moment Sum histogram for the entire earthquake record. Between July 2017 – April 2019, earthquakes become more frequent between April 2018 – September 2018, then remains generally inactive till March 2019 (Fig. 11). In September 2018, there is also a spike in the daily moment sum. This spike in the daily moment sum is ~80% stronger than the plot

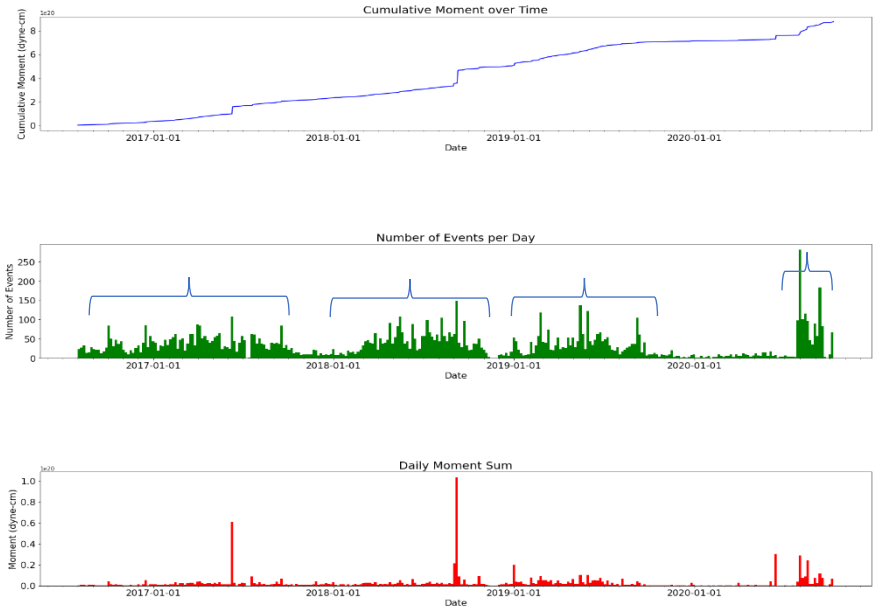

Figure 10: Cumulative Moment, Number of earthquakes per day, Daily Moment Sum within 1.5 km of Main Endeavour Field. Between August 2016 to October 2020.

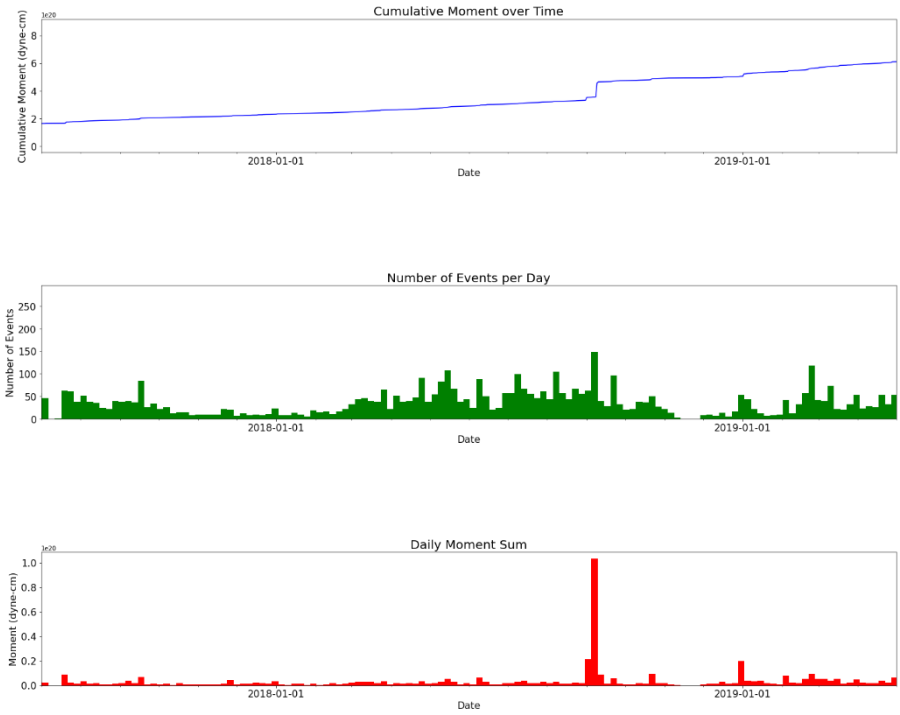

Figure 11: Earthquake data between July 2017 to April 2019.

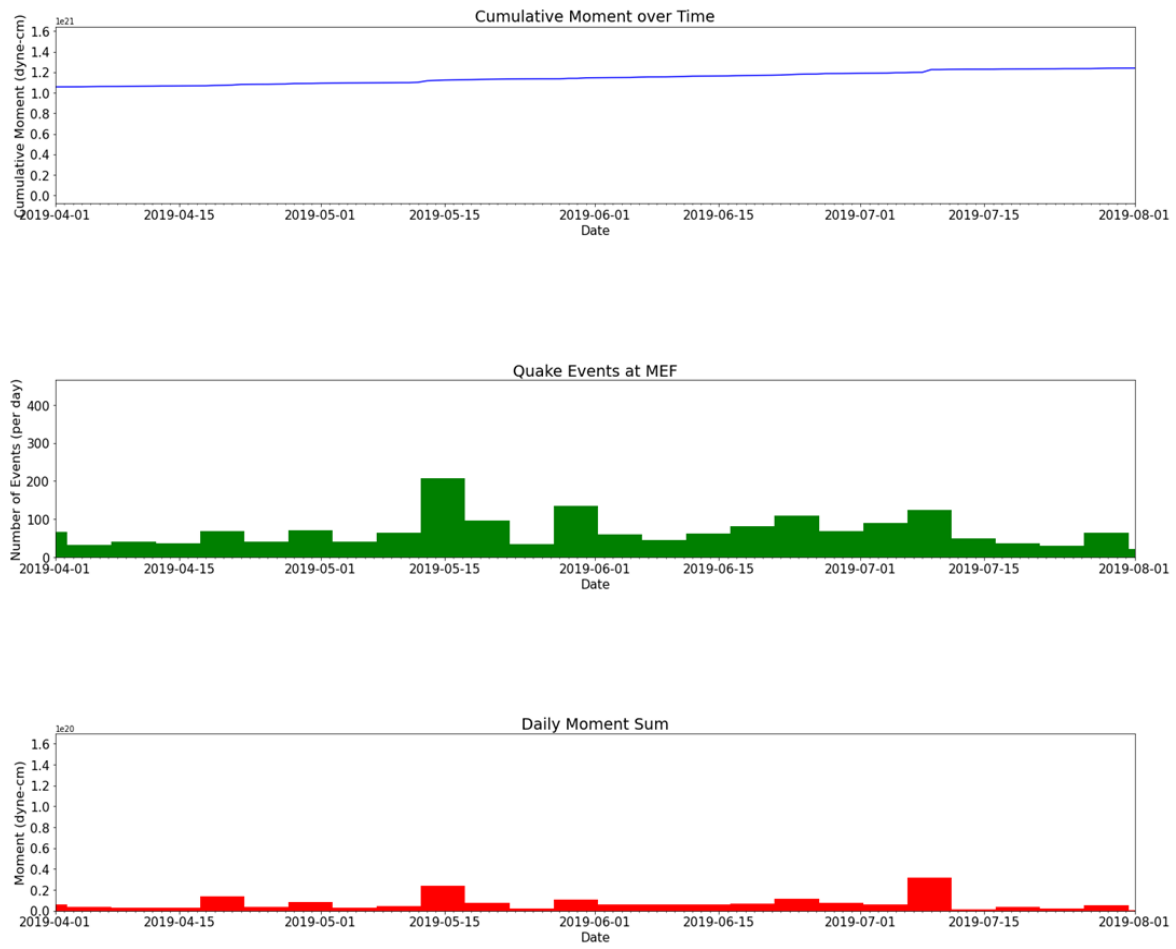

Figure 12: Earthquake data between April 2019 to August 2019.

average. April 2019 – August 2019, earthquake's cumulative moment increased ~15% (Fig. 12). The overall number of events per day averaged ~90 quakes. The largest single day event sum occurred on May 15, 2019 with 200 events. Daily moment sum average is ~2.61 x 10^{17} dyne-cm with a significant spike on May 15, 2019 and July 9, 2019.

Discussion:

When comparing each data set side-by-side, it does look as if seismic activity plays a direct and indirect role in vent temperature and resistivity. The drastic decrease in temperature at the beginning of 2020 and the following single day increase is likely results from the BARS

falling (Fig. 6). Therefore, data after January 2020 was not reliable enough to include in my study. Based on the original timeline I found that the temperature increase that begins mid-May 2019 (Fig. 5), appears to be simultaneous to the earthquake event increase on May 15, 2019, as well as the spike in earthquake moment sum (Fig. 11). However, it is difficult to say that this correlation unquestionably supports my hypothesis. Although there is a temperature increase during a spike in event and moment, the gradual and steady increase may indicate that a single event is enough to increase temperature over an extended period instead of simultaneously linked to single day events. After the spike in events on May 15th, events decrease by 100 events over the next few days, and then another 75 events several days after that. If the temperature was directly attributed to single day events, I would have expected temperature to show some sort of decrease by at least July. However, that is not the case in figures 5 and 9.

For the data between April 2019 – August 2019, resistivity and earthquake relationship does not seem to be as obvious as temperature's relationship. It looks like the resistivity data is extremely sensitive to other factors possibility outside of earthquake influence. However, the data may prove that resistivity daily averages are a result of the energy created from earthquake moment. Looking at only the resistivity plot, there are four significant voltage changes (Fig. 9). Each one of these changes in resistivity seems to line up with parts of the month that has an increase of daily moment sums. Where there are increases in voltage, there are also increased daily moment sums. Concurrently, where there are decreases in voltage, there are also decreased daily moment sums. This comparison is only for the general average taken between periods of a month or a month and a half. Resistivity fluctuations on what seems to be a bi-daily schedule. These fluctuations are possibly caused by factors that are not related to seismic activity.

Around August 2018, earthquake activity averages ~50 earthquakes per day until November 2018. Mid – October 2018, there is a single day that had ~100 earthquakes which occurred that day. The general earthquake activity between August 2018 – November 2018, and the single day event of ~100 quakes, seem to line up with the gradual temperature increase between the same dates. Shortly after the period of increase, both temperature and quake activity decrease until April 2018. The temperature seems to be significantly affected by the lack of earthquake activity and results in the largest temperature decrease up to this point. From April 2018 – November 2018, earthquake frequency begins to increase again. There are several days between this time-period where there are spikes in daily events, but it is nothing drastic. However, there is a significant increase in the daily moment sum. The overall earthquake frequency does seem to aid temperature increase over a period of several months, but the daily moment sum spike does not appear to increase the temperature as I expected. In fact, temperature does not look to be affected by the daily moment sum spike at all. Overall, adding this extended timeline appears to confirm temperature is more affected decreased earthquake activity than increased activity or the daily moment sum increases. In both timelines, temperature decreases rapidly once earthquake activity decreases, but then there is a lag in the temperature increase when earthquake activity increases again.

Due to unreliable resistivity data, I was unable to interpret this property until July 2018. Looking at a longer time-period for resistivity makes my assumption less confident than before that earthquakes have a direct and/or indirect affect towards it. Resistivity does appear to follow the general trend of increased earthquake activity equals increased resistivity; however, resistivity has several major fluctuations that are not consistent with the earthquake data. I do

believe that this confirms my assumption that other factors, other than earthquake activity, are affecting resistivity.

Conclusion:

Knowing how seismic activity affects hydrothermal vent properties could help determine what is happening to vent chemistry and the surrounding biological environment post-earthquake. If it is proven that temperature fluctuates due to seismic activity, then it may be possible to determine the severity of fluctuations based on energy produced. As a result, that understanding of temperature change can be applied to vent chemistry and how volatile species will react. Additionally, much like temperature, volatile species will react differently based on resistivity since it is a function of both temperature ad salinity. If both correlations can be proven, then this knowledge can be applied to known biological species that live near these vents and help identify if survivability is not possible after increased number of events, or decreased, and also the strength of earthquakes. If it is known that certain organsms can only survive at certain temperatures, then it can be assumed that they will be affected by increased earthquake activity via ocean water temperature change.

From my research, it does seem that there is direct and indirect correlations between earthquakes and vent properties. It is difficult to say either are undeniably proven due to other factors that may be playing a role in temperature and resistivity fluctuations. Temperature does change when there is increased seismic events, but not always. Additionally, resistivity does change what seems to be based on strength of earthquakes. However, resistivity oscillates on almost a daily basis and does not seem to be attributed to earthquakes.

I believe that this research should be continued but on a larger scale and varying locations if possible. The extension of my original timeline provided greater insight on both temperature and resitivity which improved my overall understanding of how both properties were affected. What made this study more feasible than maybe some areas, was the use of NEPTUNE. However, even without the use of a structure similar to NEPTUNE, this study can and should be duplicated at other hydrothermal vent fields.

Acknowledgements:

I want to thank Professor Mark Warner for being my mentor and instructor while working on my thesis, and Professor William Wilcock for giving input on topics, methods, and discussion. I want to thank Zoe Krauss for compiling, calculating, and disseminating the earthquake catalogue, as well as, help with Python coding. Lastly, I want to thank Ocean Networks Canada for collecting and publishing temperature and resistivity data from NEPTUNE.

References:

Coogan, L. A., Attar, A., Mihaly, S. F., Jeffries, M., Pope, M. (2017). Near-vent chemical processes in a hydrothermal plume: Insights from an integrated study of the Endeavour segment. *Geochemistry, Geophysics, Geosystems, 18*(4), 1641-1660. doi:10.1002/2016gc006747

Ding, K., Seyfried, W., Tivey, M., Bradley, A. (2001, April 02). In situ measurement of dissolved H2 and H2S in high-temperature hydrothermal vent fluids at the Main Endeavour Field, Juan de Fuca Ridge.

Kelley, D., Carbotte, S., Caress, D., Clague, D., Delaney, J., Gill, J., . . . Wilcock, W. (2012). Endeavour Segment of the Juan de Fuca Ridge: One of the Most Remarkable Places on Earth. *Oceanography, 25*(1), 44-61. doi:10.5670/oceanog.2012.03

Krauss, Z., Wilcock, W., Heesemann, M., Kukovica, J., Schlesinger, A., Farrugia, J. (2020, December 16). Understanding the seafloor spreading cycle at the Endeavour Segment, Juan de Fuca Ridge using a multi-decadal microearthquake catalog.

Seewald, J., Cruse, A., & Saccocia, P. (2003). Aqueous volatiles in hydrothermal fluids from the Main Endeavour Field, northern Juan de Fuca Ridge: Temporal variability following earthquake activity. *Earth and Planetary Science Letters, 216*(4), 575-590. doi:10.1016/s0012-821x(03)00543-0

Tsurumi, M., & Tunnicliffe, V. (2003). Tubeworm-associated communities at hydrothermal vents on the Juan de Fuca Ridge, northeast Pacific. *Deep Sea Research Part I: Oceanographic Research Papers, 50*(5), 611-629. doi:10.1016/s0967-0637(03)00039-6

Wilcock, W.S., E.E.E. Hooft, P.R. McGill, D.R. Toomey, A.H. Barclay, D.S. Stakes, and T.M. Ramirez. 2007. Microearthquakes beneath the Endeavour hydrothermal vent fields: Insights into reaction zone processes. Eos, Transactions, American Geophysical Union 88(52): Fall Meeting Supplement Abstract S13F-02